18th Australasian Fluid Mechanics Conference
Launceston, Australia
3-7 December 2012

Hot-wire Calibration at High Subsonic & Transonic Mach Numbers

J. H. Watmuff[1], M. B. Jones[2], S. M. Henbest[2] and A. Blandford[2]

[1]School of Aerospace, Mechanical and Manufacturing Engineering, RMIT University, Bundoora, Victoria, 3083 Australia
[2]Air Vehicles Division, Defence Science and Technology Organisation, Melbourne, Victoria, 3207 Australia

Abstract

A technique has been developed to change the Resistance Ratio (*RR*) of a constant–temperature hot–wire anemometer: while it is operating; under electronic control; and at relatively high frequencies. The technique has been implemented by modifying anemometers built at DSTO that follow the design of Watmuff [3]. The modifications include adding a device for electronic switching of additional bridge resistors in parallel with the balance resistor, R_b. Severe large–amplitude transients are observed as a result of the switching even for moderate changes in *RR*. However, these large–amplitude transients contain very high frequency components and they have a corresponding rapid decay rate and they appear to be benign in the sense that there has not been any noticeable increase in hot-wire breakage. Observations demonstrate that the *RR* switching also introduces lower frequency components that appear to be identical to the usual electronic square wave response that is used to tune constant–temperature anemometers. A theoretical model for the transient behaviour using a similar generalized Laplace transform method to Watmuff [2] remains to be derived. Calibration data at high subsonic and transonic Mach numbers have been obtained in the DSTO Transonic Wind Tunnel (TWT). The benefit of high–speed dynamic alternation of *RR* is that the calibration and application data points for multiple *RR* can be obtained using a single measurement realization. Furthermore, almost identical flow conditions are experienced at each *RR* compared to the conventional method where data are obtained as independent realizations at each *RR*.

Introduction

For more than 75 years the constant–temperature anemometer has been used in subsonic flow and more recently it has been used successfully in supersonic flow. However, hot-wires have not been used extensively in transonic flows, partly because the large dynamic pressures in transonic flows tend to cause wire breakage and partly due to difficulties with the calibration. The main problem with calibration in transonic flows is that the sensitivities to velocity and density fluctuations both depend on Mach number and Reynolds number.

In subsonic incompressible flow the heat transfer from a wire is a function of the mass flow, total temperature and the wire temperature. However, the density is effectively constant at low Mach numbers so that all of the mass–flow variations can be attributed to velocity fluctuations. The Nusselt number is assumed to be a function of the Reynolds number and the Prandtl number alone. In most applications the Prandtl number can be assumed to be constant, which leads to the familiar King's law calibration.

The effects of fluid compressibility on the heat transfer from the wire must be taken into account at higher speeds. In supersonic flow it was discovered experimentally that the heated wire is sensitive only to mass flow and total temperature. The reason for this behaviour is that a strong bow shock is located upstream of the wire in supersonic flow. Therefore the wire is operating in the locally subsonic flow downstream of the shock.

At high–subsonic and transonic Mach numbers the heat transfer from the wire is a function of velocity, density, total temperature, and the wire temperature, *i.e.* $\mathrm{Nu} = f(Re, M, \theta)$. Because of this complexity, these flow regimes were largely ignored until the 1970's and 1980's when attempts were made to develop methods applicable for these flows.

A proper and full hot-wire calibration in compressible flow requires a facility in which the density, total temperature, and the velocity can all be varied independently of each other. The DSTO Transonic Wind Tunnel (TWT) offers much of this capability, and calibration data has been obtained over a range of Mach numbers; $0.3 < M < 1.2$ and total pressures; $45 < P_0 < 155$ kPa. A substantial benefit of the TWT is the reasonably good control over constant total temperature, *i.e.* $\pm 1^\circ K$, which has simplified the development of calibration schemes.

Anemometer Design and Modifications

Watmuff [1] conducted an investigation into hot-wire behaviour which was motivated by observations of hot-wire behavior in supersonic flow at the Gas Dynamics Laboratory at Princeton University. The results of a 5^{th}–order analysis showed that the so-called phenomenon of strain-gauging is most likely a purely electronic, rather than an electro-mechanical phenomenon. Watmuff [2] completely generalized his original analysis and developed an algorithm for deriving the transfer functions of the constant temperature hot-wire anemometer of arbitrary complexity. He demonstrated that a minimum of two equivalent amplifiers are required to model the feedback amplifier properly. He showed that in general, the poles of the transfer functions for electronic and velocity perturbations will always be identical, regardless of complexity of the system, the frequency response characteristics of the feedback amplifier and the nature and quantity of components used to model the bridge impedances. The feedback amplifier must have the potential for both a high gain and a high frequency response in order for the system as a whole to achieve stable high frequency operation.

Practical constant temperature hot-wire anemometer designs should use a cascade of amplifiers rather than a single feedback amplifier because of the gain-bandwidth product limitations of physical devices. A cascade of n amplifiers is used in the model shown in figure 1. These and other theoretical considerations led to a practical design which is specified in detail in the NASA Contractor Report by Watmuff [3]. The report provides details, such as fabrication drawings and a parts list, to enable the instrument to be constructed by others. The design allows the highest possible frequency response while maintaining system stability. Further enhancements include the use of two modular power supplies to achieve a high signal-to-noise ratio. A total of 40 anemometers were built at NASA Ames Research Center based on this design.

A total of four of these hot-wire anemometers have been built at DSTO using the same chassis and PCB design as specified by Watmuff. Under transonic flow conditions, *e.g.* $M = 0.5$ and $p_0 = 120$ kPa, the use of a "standard" 5 micron diameter 1 mm long tungsten hot-wire filament led to anemometer output volt-

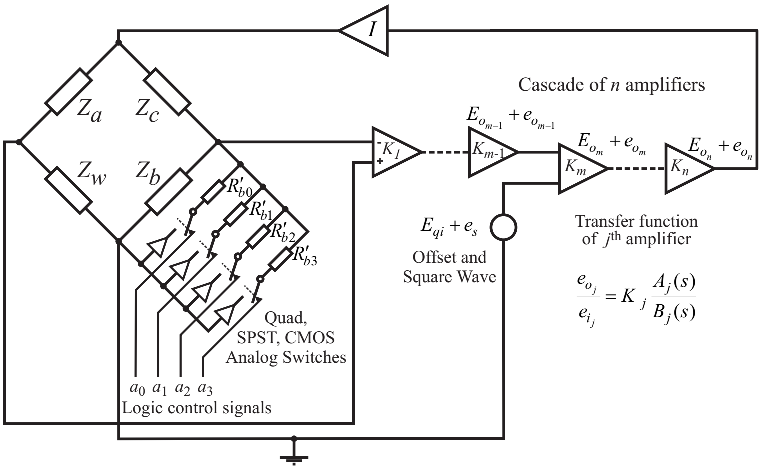

Figure 1: Schematic of constant–temperature hot–wire anemometer with four remote controlled CMOS analog switches for connecting additional resistors in parallel across the balance resistor, R_b, to allow high frequency multiplexing of Resistance Ratio.

ages in excess of 12 volts causing saturation of the operational amplifiers. Consequently, the upper bridge resistors (refer to figure 1) in the DSTO implementation have been reduced from $R_a = 100\Omega$ and $R_c = 1000\Omega$ to $R_a = 40\Omega$ and $R_c = 400\Omega$. With this setup the same "cross-bridge" resistance ratio of 1:10 is maintained. The reduction in magnitude of the upper bridge resistors reduces the magnitude of the anemometer output voltage by around 50% thereby avoiding saturation of the amplifiers.

Activation of the additional balance resistors which change the *RR* is performed using a device (Maxim, MAX4665) which contains four CMOS analog switches. These switches have 5Ω maximum on-resistance and they can operate at a maximum switching frequency in excess of 10 MHz. Therefore the *RR* could be switched at a frequency of order of the frequency response of the anemometer (*e.g.* at 20 to 60 kHz). The additional balance resistors can be inserted individually in parallel to the balance impedance, Z_b, under electronic control using the logic level signals. Insertion of a parallel resistor will reduce the magnitude of the balance resistor and hence reduce the Resistance Ratio, *RR*, thereby minimizing the risk of wire breakage. The advantage of this approach is that the anemometer does not have to be switched off while the *RR* is changed.

Thermal expansion introduces a small bow in wire shape. Sustained high frequency application of step changes in *RR* (wire temperature) might be expected to cause premature fatigue failure of the wires. However, initial tests using an approximately 20% alternation of *RR* at 40 Hz over a 70 h period ($\sim$10M cycles) with zero flow did not cause wire breakage. We have not experienced any increase in wire breakage while using the dynamic *RR* alternation technique under transonic flow conditions.

A total of 16 *RR* settings can be selected by using all permutations and combinations of the four analog switches. The largest *RR* will occur when none of the additional bridge resistors are connected in parallel, and the smallest *RR* will occur when all of the additional bridge resistors are connected in parallel across the balance resistor. It turns out that using a geometric series for the magnitude of successive additional balance resistors leads to a reasonably linear variation in *RR* over the full range of the ordered logic levels. Results are described below which demonstrate that large–amplitude transients are generated when the resistance ratio is changed. Therefore one of the design objectives is to minimize the *RR* step-size during the switching sequence. Alternate values of the ordered sequence can be used for the first half of the switching sequence, where *RR* is reduced, and for the second half of the sequence, where *RR* is increased, leading to small step-size variations of *RR*. An example of the alternate *RR* stepping sequence is shown in figure 2 Determination of the sensitivity at different *RR* provides a means to distinguish between rms mass flow fluctuations, $(\rho.U)'$ and rms Mach number fluctuations, M'.

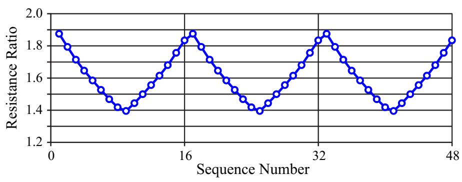

Figure 2: Alternate values of the ordered switching sequence used to obtain small step-size resistance ratio variations using the nearest available standard resistor to a geometric series. Three cycles of the sixteen resistance ratios are shown.

Results

Severe transients and a highly nonlinear response are observed during the switching, even for small changes in *RR*. Independent tests have been conducted using a circuit consisting of simple resistive components and the analog switches were not found to introduce any significant nonlinearity or transient oscillations or any other anomalous behaviour.

Nonlinearity and Transients During Switching

The most extreme nonlinearity (asymmetry) occurs under zero velocity conditions as shown in the time series in figure 3. These results correspond to the switching of a single additional balance resistor at a frequency of 40 Hz leading to alternation of *RR* by 14.8% in figures 3 (a) & (b) and 7.7% in 3 (c) & (d). These measurements were obtained using a digitizer with a range of ±10 V and the data were acquired at 200 kHz while the wire was fixed inside a small container. A limited range of the time series in the vicinity of the switching is shown in each figure.

The usual electronic square–wave response under these conditions is shown in figure 3(e). Only a slightly nonlinear (asymmetrical) response is evident in the square–wave response. However the signals corresponding to positive and negative changes in *RR* are so asymmetric that they bare almost no resemblance to each other.

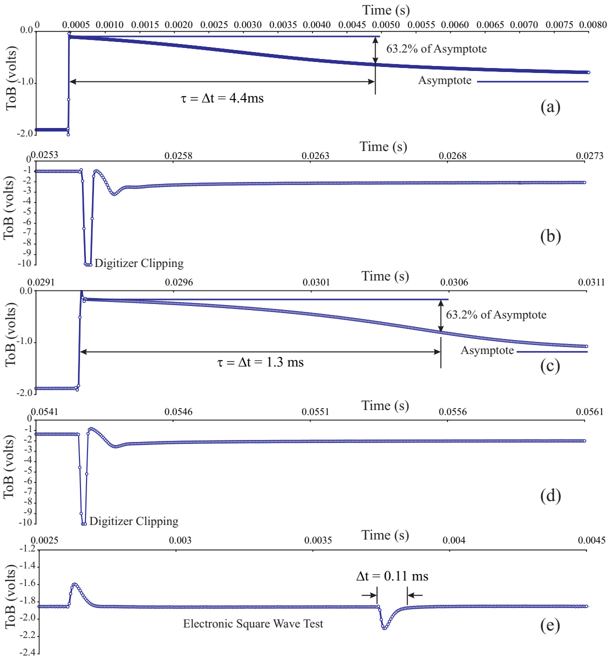

Figure 3: Severe transients and nonlinear response to *RR* for zero velocity conditions using a single additional balance resistor switched at 40 Hz : (a) Switch–On: 14.8% reduction in *RR*, $\tau \approx 4.4$ ms; (b) Switch–Off: 14.8% increase back to $RR = 1.7$; (c) Switch–On: 7.7% reduction in *RR*, $\tau \approx 1.3$ ms; (d) Switch–Off: 7.7% increase back to $RR = 1.7$; (e) Conventional electronic square–wave test (without *RR* switching).

The Switch–On condition corresponds to a reduction in *RR* (wire temperature) and in both cases the transient output of the anemometer reaches an extreme value of zero volts. Examination of the signals using a high performance oscilloscope revealed that the Switch–On transition introduces very high frequency oscillations of order 10 MHz which are not captured by the digitizer. Long recovery times are required following the transition to the Switch–On condition for the anemometer output voltage to reach the asymptotic value. The time constant τ defined for an *RC*-circuit provides a useful measure of the time constant under these conditions (*i.e.* the time to reach 63.2% of steady state value). The time constants shown in the figure are an order of magnitude larger than the electronic square–wave response time. Furthermore, the time constant for recovery to a steady state signal is dependent on the magnitude of the change in *RR*.

A large–amplitude transient spike is observed during the transition to the Switch–Off condition. In both cases the spike extends to the maximum output amplitude of the anemometer. However this behaviour is not visible in figures 3(b) and (d) since the severe voltage swings have been clipped by the digitizer. The waveforms following the spikes more closely follow the electronic square–wave response.

A nonlinear (asymmetric) response is evident in the electronic square–wave when the stability is tuned by adjusting the offset voltage as shown in figure 4(c). The corresponding Switch–Off transients are shown in figures 4(a) and (b) and a similar under–damped response is observed. However, the ringing frequency is consistently higher, which is unusual since these results are obtained during the transition to a smaller *RR*.

At this stage we have not derived a theoretical explanation for these observations. However, what is important for the current work is that the anemometer is given sufficient time to recover from the transients so that the output voltage can be trusted to provide useful results corresponding to each *RR*.

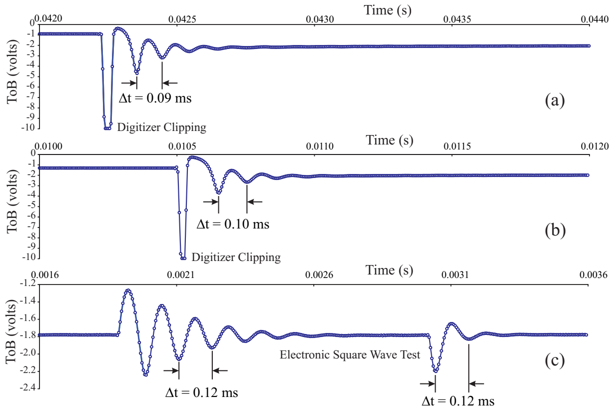

Figure 4: Detuned system. Response to *RR*, zero velocity, single additional balance resistor switched at 40 Hz : (a) Switch–Off: from a 14.8% reduction back to $RR = 1.7$; (b) Switch–Off: from a 7.7% reduction back to $RR = 1.7$; (c) Conventional electronic square–wave test (without *RR* switching).

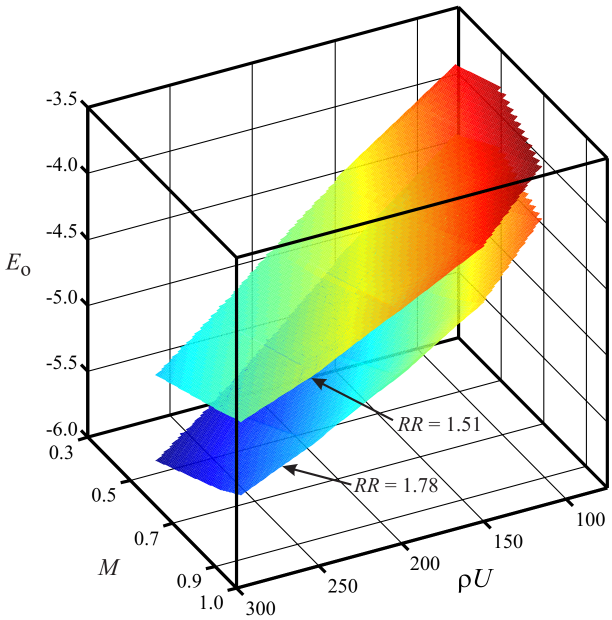

Figure 5: Static hot-wire calibration data performed in the DSTO Transonic Wind Tunnel using a 5 micron diameter, 1 mm long tungsten hot-wire filament manually switched between $RR = 1.51$ and $RR = 1.78$.

Calibration at High–Subsonic and Transonic Speeds

Static calibration data for a 5 micron diameter 1 mm long tungsten hot-wire filament are shown for two *RR* in figure 5 over a wide range of operating conditions Note that the anemometer output voltage is negative. The calibration is termed static because the *RR* was held constant at each of the 36 calibration points while the data for each *RR* was obtained. The *RR* was changed by using a manually operated toggle switch to drive one of the logic inputs of the quad analog switch shown in figure 1. The average anemometer output voltages were evaluated from data averaged over a 10 s period. The magnitude of the single additional balance resistor was 562Ω, leading to a configuration with the $RR = 1.78$ with the R_b alone and $RR = 1.51$ with the additional balance resistor (14.8% reduction).

The 36 calibration points have a reasonably uniform distribution over a range of Mach numbers, $0.3 < M < 1.0$, and total pressure, $45 < p_0 < 155$ kPa, leading to a freestream mass flow variation, $75 < \rho.U < 300$ kg/s. A least–squares second–order polynomial surface of best fit has been applied to both mass-flow $\rho.U$ and Mach number M and it has been found to fit the anemometer output voltage very well over this parameter range. Note that the absolute sensitivity of the anemometer output voltage to Mach number is negative, *i.e.* increasing the Mach number leads to a reduction in the absolute voltage, while the sensitivity to mass flow variations is positive.

Concurrent Calibration using the Switching Technique

Performing the dual parameter static hot-wire calibration shown in figure 5 required a total time of approximately 8 h to set and stabilize operation of Transonic Wind Tunnel at each of the 36 calibration data points. The calibration has been repeated using the switching technique but over a more limited range of Mach numbers, $0.5 < M < 0.7$, and total pressure, $72 < p_0 < 145$ kPa, leading to a freestream mass flow variation, $150 < \rho.U < 250$ kg/s. This is approximately half the Mach number and total pressure range used for the static calibration shown in figure 5. A similar distribution spacing has been used, but the reduced range means that only nine data points are required. Results are obtained using the very small amplitude switching range of RR of 1% and 2%.

The phase-averaging process has been applied to the hot-wire signals. The switching frequency is 200 Hz and the data are sampled at 200 kHz. Example phase-averaged hot-wire results for one of the nine calibration points is shown in figure 6(a) and (b). Minor distortion is introduced since exact synchronization does not exist between the switching and data acquisition signals since they were generated by different devices. However, by using a large number of phase intervals the smearing only occurs over the sample on either side of each data point and the main features are clear in the phase–averaged waveforms. It is evident that at these flow speeds and with these small amplitude changes in RR that the hot-wire signals do not suffer from the extreme nonlinearity and severe transients observed in figures 3 and 4

It is important to clearly identify the portions of the signals that will be effected by the switching transients since these portions must be excluded from the data analysis. Appropriate time periods around the switching can be identified from the calibration data. It is clear that the time records at each RR will be discontinuous. However, there is no statistical reason why discontinuous time records will not produce valid estimates of mean and rms quantities.

Conclusions

Dynamic alternation of the Resistance Ratio of a constant–temperature hot–wire anemometer has been successfully demonstrated at high subsonic and transonic Mach numbers in the DSTO Transonic Wind Tunnel. Surprisingly large–amplitude transients are observed as a result of the switching even for moderate changes in RR. However, it has been shown that transients can be made acceptably small by using small magnitudes for changing the RR. The benefit of high–speed dynamic alternation of RR is that the both calibration and measurement data can be obtained for multiple RR obtained using a single measurement realization. Further work is required to demonstrate measurements with the technique.

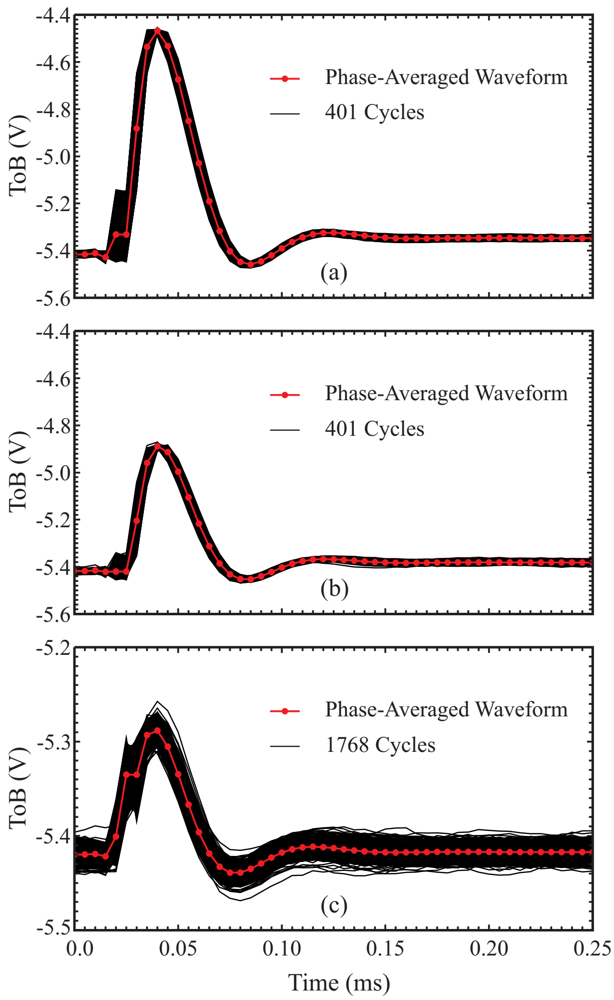

Figure 6: Small amplitude RR switching. Hot-wire signals at $M = 0.5$, $\rho.U = 200$ kg/s operating at $RR = 1.833$ with dynamic switching at 200Hz to (a) $RR = 1.813$ (-1%), and (b) $RR = 1.796$ (-2%). Data sorted into 401 cycles (solid black curves) and phase–averaged using 999 phase intervals. (c) Electronic square–wave test: Data sorted into 1768 individual cycles and phase–averaged on the basis of a signal transition threshold of 0.05 V between samples.

Acknowledgements

This work is supported by DSTO Research Agreement ID3677.

References

[1] Watmuff, J., Some higher order effects in the behavior of constant temperature hot-wire anemometer systems, in *IN: Symposium on Thermal Anemometry, Cincinnati, OH, June 14-17, 1987, Proceedings (A88-14168 03-34). New York, American Society of Mechanical Engineers, 1987, p. 25-34.*, 1987.

[2] Watmuff, J., An investigation of the constant-temperature hot-wire anemometer, *Exp Therm. & Fluid Sci*, **11**, 1995, 117–134.

[3] Watmuff, J. H., A new high performance constant temperature hot-wire anemometer., *NASA Contractor Report 177645*.